

Prediction of Pressure Losses in Pipe Flow of Aqueous Foams

B. S. Gardiner, B. Z. Dlugogorski,*[†] and G. J. Jameson

ARC Research Centre for Multiphase Processes, Department of Chemical Engineering,
The University of Newcastle, Callaghan NSW 2308, Australia

This paper presents a model for predicting pressure losses in foams of various expansions and pressures, in pipes of any given diameter, once the foam behavior has been characterized at a single expansion and pressure. The model incorporates a modified form of the power-law viscosity model of foam, which is obtained through the method of volume equalization. Since apparent wall slip contributes significantly to pipe flow of foam, the wall slip also needs to be characterized to enable predictions of pressure losses. The couplings between foam flow and wall slip characteristics are investigated, and two models are presented to predict slip velocities for slow and fast flow rates. Experimentally we find that $u_{\text{slip}} \propto \epsilon^{-3/2}$, where ϵ denotes the foam expansion ratio at the experimental pressure. Predicted results are compared with experimental observations, with good agreement.

Introduction

The use of compressed-air foam (CAF) systems to produce fire-fighting foam is growing in popularity in preference to the more traditional air-aspirated systems.^{1,2} CAFs are often used to enhance crude oil production to fracture oil-bearing formations.³ Foams are prevalent in the food industry, and in some cases food-foams, such as aerated chocolates, are pumped through pipes at elevated pressures.

Whether the application is in a warehouse, mine, or chocolate factory, the efficient design and operation of a CAF system requires a knowledge of the flow characteristics of foam through pipes. As yet, there is no method to enable the prediction of pressure losses in the pipe flow of foams, since foam exhibits many complex flow properties such as compressibility, shear thinning, elasticity, yield stress, and slippage at the pipe wall.

To make predictions of foam behavior through pipes two different, but related, phenomena need to be better understood. The first phenomena is the viscous bulk flow of foams. Foam viscosity depends on other foam properties such as the foam expansion ratio E , bubble size distribution, and properties of the individual phases. The second phenomena influencing pipe flow is the apparent slip of foam at the pipe wall. Wall slip occurs due to the foam flowing on a thin layer of liquid at the pipe wall. The wall liquid layer originates from within the foam; therefore its thickness and viscosity also depends on the properties of the foam as well as characteristics of the pipe. The effect of wall slip is to increase the expected foam flow rate and to make the apparent foam flow behavior pipe-diameter dependent.

In rheometric experiments using the Poiseuille rheometer, also called pipe rheometer, the effect of wall slip can be removed from the flow data by following the method of Oldroyd⁴ and Jastrzebski.⁵ In combination, the Poiseuille rheometer and the method of Oldroyd and Jastrzebski allows both foam viscosity and wall slip to be investigated in a geometry of interest to the many industrial applications of CAFs.

To describe the flow behavior of CAFs used in the petroleum industry, Valkó and Economides⁶ introduced the method of volume equalization. The method of volume equalization incorporates foam compressibility to account for changes in foam flow behavior associated with a change in pipe pressure and foam gas volume fraction. The result of the method of volume equalization is that the flow data for foams at different pressures and gas concentrations can be reduced to a master equation relating foam stress to the shear rate.

With the emerging widespread use of CAFs there is a need for predicting conditions under which a stable foam will flow and still maintain its desirable properties. By using the results of the volume equalization technique coupled to foam wall slip behavior, the following sections of this paper show how the pressure losses in the flow of foam in a pipe can be predicted.

Foam Viscosity and Volume Equalization

The true rheology of aqueous foam has been hidden in many past foam viscosity experiments due to the confounding effects of wall slip, variation in foam structure with foam age, and mode of foam generation.⁷ However, many general characteristics of foam rheology are known. Foams display shear-thinning behavior^{8–14} and often a yield stress is reported;^{8,11,15–17} hence, typically a Herschel–Bulkley model is fitted to experimental flow data.

Table 1 lists the results of several experiments on foam rheology in which some attempt has been made to reduce the effects, on foam rheology, of wall slip and foam structure evolution. Although results listed in Table 1 are for foams of differing properties such as surface tension, liquid-phase viscosity, and bubble size distribution, there are several trends that can be inferred.

The fitting of a model containing a yield stress component to the experimental results is more likely to occur if the experiments include low shear rates data. For experiments conducted at higher shear rates, typical of industrial processes, a simple power-law model is sufficient. For all experiments reported, foam was seen to exhibit shear-thinning behavior. Although not clear in Table 1, due to the effects of bubble size and surface

[†] E-mail: cgbzd@alinga.newcastle.edu.au. Ph: +61 2 4921 6176. Fax: +61 2 4921 6920.

Table 1. Summary of Published Past Foam Viscosity Data and the Models Used To Fit the Data

authors	expansion ratio, ϵ	shear rates (s^{-1})	fitted model	k ($Pa\ s^n$)	n	τ_y (Pa)
Wenzel et al. ⁸	38–250	0.2–18	$\tau = \tau_y + k\dot{\gamma}^n$	1.73–6.8	0.13–0.69	1.32–12.05
Thondavadl and Lemlich ⁹	8.3–100	0.2–6.2	$\tau = k\dot{\gamma}^n$	1.43	0.61	
de Krasinski and Fan ¹⁰	10–17	0.05–500	$\tau = k\dot{\gamma}^n$	18.5	0.5	
Khan et al. ¹¹	12.5–33	0.01–0.5	$\tau = \tau_y + k\dot{\gamma}$		1	13.5–17.5
Enzendorfer et al. ¹²	1.92–3.3	5–1000	$\tau = k\dot{\gamma}^n$	2.5	0.34	
Boissonnet et al. ¹³	5–6	10–10 000	$\tau = k\dot{\gamma}^n$	0.26	0.6	
Gardiner et al. ¹⁴	4.4–7.5	10–1500	$\tau = k\dot{\gamma}^n$	2.29	0.29	

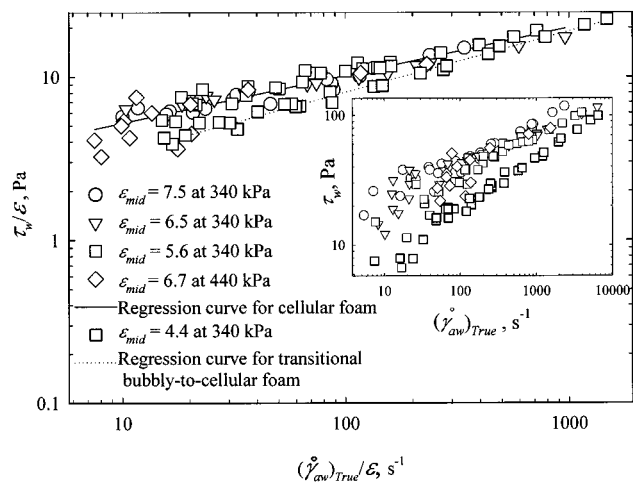


Figure 1. All flow data of Gardiner et al.¹⁴ corrected for wall slip and volume equalized. Once the original slip corrected flow data appearing in the inset are volume equalized, the data trace one of two curves relating to either polyhedral foam $\epsilon_{mid} > 5$ or bubbly transition foam $4 < \epsilon_{mid} < 5$. The transition foam reflects a foam whose properties are not dominated by either thin films (as for cellular foams) or by an abundance of liquid (as for gas dispersions/bubbly foam). This means that the transition between the rheological behavior of bubbly and cellular foam is not sharp.

tension variations among authors, each set of data shows an increase in the apparent foam viscosity with the expansion ratio.

Despite the trends seen experimentally, there is still no empirical relationship between foam viscosity and the many possible variations in the foam structure and the properties of the liquid and gas phases. Current foam models are unable to predict the rheological behavior of any given foam. However, some advancement has been recently achieved by applying the method of volume equalization.

Valkó and Economides⁵ first introduced the method of volume equalization to describe the flow behavior of CAFs used in the petroleum industry. At elevated pressures within a pipe, the expansion ratio (E , measured at atmospheric pressure) ceases to be a useful parameter as the volume of gas contained in the foam is strongly dependent on the pipe pressure. Instead Valkó and Economides hypothesized that a more suitable parameter would be the specific expansion ratio ϵ . The method of volume equalization developed by these researchers implies that the flow data, for foams characterized by a range of E at various pressures, can be reduced to a master equation relating foam stress to the shear rate, with the help of ϵ . The method of volume equalization has been verified with pipe flow data of power-law shear thinning foams by various authors.^{12–14}

To illustrate the capabilities of the method of volume equalization, the final experimental results of Gardiner et al.¹⁴ are shown in Figure 1. Flow data shown in Figure 1 were obtained from observations of pressure

losses in pipes of various diameters, $D = 6.95, 9.9,$ and 15.8 mm. The range of pipe diameters allowed the foam slip at the pipe wall to be determined and removed from rheological results by following the method of Oldroyd and Jastrzebski. See Gardiner et al.¹⁴ for more detail on the method of foam generation and slip correction. Figure 1 illustrates that prior to volume equalization the data obtained from experiments at various pressures and foam expansions do not fall on a single master curve (Figure 1 inset). However when volume equalized, flow data trace one of two separate master curves depending on whether the foam consists of cellular structure or whether the foam contains spherical bubbles. This result is the first step toward the prediction of pressure losses of foam flow in pipes as it allows a single viscosity expression to be used for the foam, over a range of pressures and expansions, once the foam has been characterized at a single pressure and expansion ratio.

Wall Slip

The second main hurdle in being able to predict pressure losses associated with the flow of foams is the lack of a full understanding of the functional dependence of apparent wall slip of foams on pipe and foam properties. The phenomenon of wall slip is a useful approximation when modeling the flow of foam. In reality foam flows on a thin liquid layer at the pipe wall, of thickness δ , which is much smaller than the pipe diameter, D . Typically δ is of the same order as the interbubble film thickness for polyhedral bubble foams, that is $1–30\ \mu\text{m}$.^{9,17,18}

Ultimately the liquid layer at the pipe wall has originated from the foam and hence its thickness and properties are coupled not only to pipe roughness, diameter, and foam shear rate but also to foam properties such as surfactant concentration, dispersed-phase concentration, bubble size distribution, and liquid-phase viscosity. The following section briefly discusses past experimental observations and investigates possible models for predicting wall slip behavior.

As with other materials displaying wall slip, many of the earlier experiments on foam rheology were affected by wall slip. If the slip was not accounted for in the data analysis, experimental results were often geometry-dependent. Before accurate predictions of pressure losses in practical foam applications can be made, a greater understanding of the sensitivity of wall slip velocity and slip layer thickness to the properties mentioned above needs first to be established.

Thondavadl and Lemlich⁹ found that in smooth acrylic pipes the slip velocity dominated the flow of foam, whereas in rougher galvanized pipes no slip was apparent. A slip yield stress has been observed,^{8,19} below a very low wall stress, and is believed to be an effect of wall roughness. In the case of concentrated emulsions, Princen¹⁹ observed that this slip yield stress increased

with decreasing drop size. Small bubbles are able to lock into bumps in a pipe wall restricting any slip until the stress is large enough to overcome the barriers. For the same level of wall roughness, larger bubbles are less likely to be locked into position by the wall roughness.

One method which has been used successfully to account for wall slip in foams flowing in a pipe geometry is that of Oldroyd and Jastrzebski.¹² Jastrzebski⁵ extended the method of Oldroyd⁴ and applied the results to structured fluids such as concentrated suspensions of paste consistency. The Oldroyd and Jastrzebski method, more appropriate to structured fluids than the more common Mooney method,²⁰ accommodates the dependence of the slip velocity on the pipe diameter into a correction function. The Oldroyd and Jastrzebski method also provides an indirect method of studying wall slip of foams, by examining the modified wall slip coefficient (fluidity) β_c , defined by

$$u_{\text{slip}} = \frac{\beta_c \tau_w}{D} \quad (1)$$

where τ_w denotes the shear stress at the wall and u_{slip} is the slip velocity. By investigation of β_c over a range of foam and pipe characteristics, the coupling between foam properties and the slip velocity may be observed. Expressions relating β_c to u_{slip} will be used later in pressure-loss prediction equations.

An investigation of the slip coefficient as a function of wall stress for various shear rates and foam types covered by previous studies^{8,9,12,14,19} reveals a number of qualitative trends of wall slip in foams. At low shear rates ($<20 \text{ s}^{-1}$), and when ϵ is above the critical transition between spherical and polyhedral bubbles, as described by Wenzel et al.,⁸ Thondavadi and Lemlich,⁹ and Princen,¹⁹ the slip coefficient increases with shear stress (shear rate). If the stress within the slip layer is given by

$$\tau_w = \frac{\mu u_{\text{slip}}}{\delta} \quad (2)$$

it can be seen that the slip layer thickness increases with the slip coefficient, by substituting eq 2 into eq 1. If the slip coefficient increases with shear stress,^{8,9,19} then this means that the slip layer thickness also increases with shear stress.

Thondavadi and Lemlich⁹ report an upper limit to the slip film thickness. With increasing shear rate more liquid is dragged out of the thin films and Plateau borders of the foam in contact with the wall. However above a certain shear rate, the liquid in these reservoirs supplying the slip layer is depleted. It is then necessary for this liquid to come from increasingly distant regions within the foam. Hence, the supply rate of liquid to form the slip layer cannot meet demand, and the fluidity may reach a plateau or even decrease with increasing shear rate, if the pipe wall is not given sufficient wetting time. This plateau effect can be observed in the results of Thondavadi and Lemlich⁹ and Enzendorfer et al.¹² For the very high shear rates of Gardiner et al.,¹⁴ the slip coefficient was seen to decrease with wall stress; see Figure 2.

The expansion ratio plays a major role in determining wall slip behavior. Clearly the more liquid that is contained in the foam, the more liquid there is potentially available to form a slip layer. Therefore it is expected that the slip coefficient is larger for low

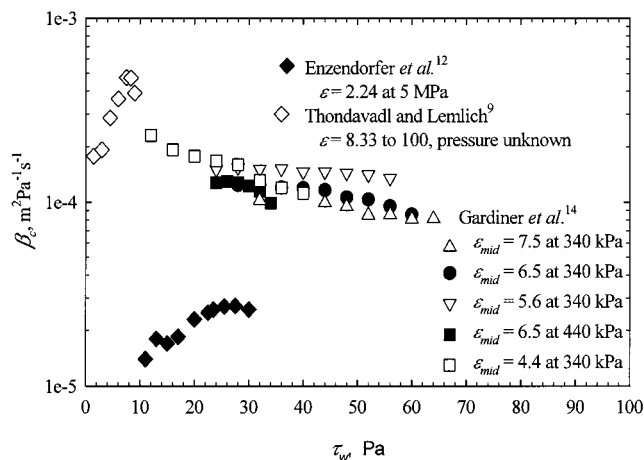


Figure 2. Collation of slip coefficients determined for three separate experimental studies. Both Wenzel et al.⁸ and Enzendorfer et al.¹² observe a slip coefficient that increases with wall stress up to a limiting stress. At the high shear rates of Gardiner et al.¹⁴ the slip coefficient was observed to decrease with wall stress.

expansion foams than high expansion foams. It is not surprising then that a decrease in the slip coefficient for high expansion foams and concentrated emulsions has been observed experimentally.^{14,19} In particular, for foams of expansion between 5.6 and 7.5, Gardiner and co-workers²¹ found the fluidity to be a function of $\epsilon^{-3/2}$. In other words, when the slip coefficient is scaled by $\epsilon^{-3/2}$, the values of the slip coefficient collapse to a single curve for the range of ϵ examined in the present study; see Figure 3. Therefore we can define an ϵ -independent β_{ce} according to the following expression

$$\beta_c = \frac{\beta_{ce}}{\epsilon^{3/2}} \quad (3)$$

The theoretical prediction of wall slip in foams is still an unsolved problem. Below, we present an attempt to provide an explanation for the scaling relationship shown in eq 3.

Kraynik,²² in considering the wall slip of a 2D, monodisperse foam system exhibiting steady flow, arrived at the relationship

$$\left(\frac{\mu u_{\text{slip}}}{\sigma}\right)^{1/3} = \frac{6.02 \alpha \tau_w (\epsilon - 1)^{1/2}}{\sigma \epsilon^{1/2} f} \quad (4)$$

where f is the fraction of the pipe wall covered by thin films. Equation 4 assumes that the stress within the thin films between the foam and the pipe wall is the main contributor to the stress associated with wall slip. For 2D stationary foams f can be obtained analytically, as done by Princen,^{19,23}

$$f = \frac{\epsilon^{1/2} - 3.28}{\epsilon^{1/2}} \quad (5)$$

Kraynik²² assumed that eq 5 also holds for a flowing foam. This assumption has not been validated and remains an open research problem.

Kraynik's expression (eq 4) largely draws on the work of Bretherton²⁴ to obtain an equation for the thickness of the slip layer film. Bretherton studied the motion of long bubbles in tubes to obtain the velocity of the fluid phase relative to the bubble velocity. As a consequence

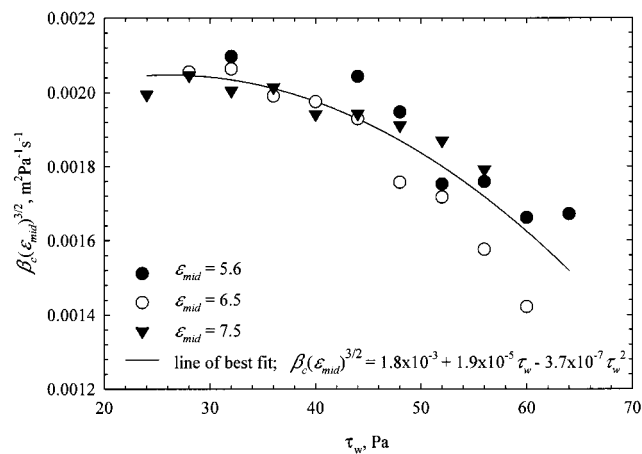


Figure 3. When Gardiner et al.'s¹⁴ constant pressure slip coefficient results are scaled by $(\epsilon_{\text{mid}})^{3/2}$, the data from three expansions can be fitted to a single curve.¹⁹

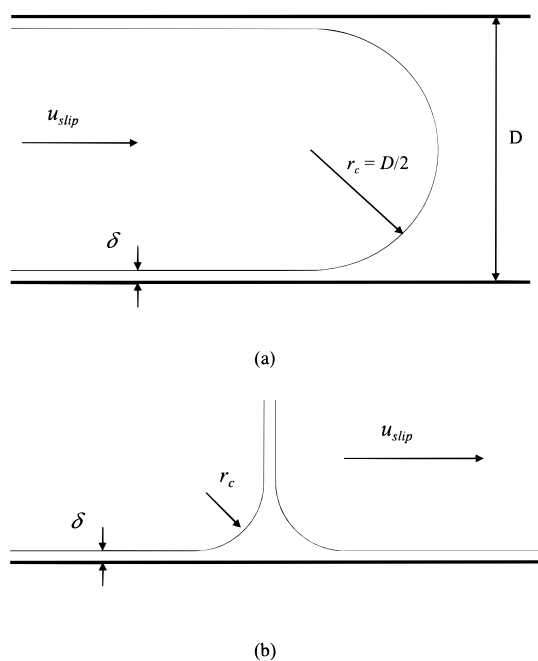


Figure 4. Illustration of (a) Bretherton's²⁴ analysis of the flow of a long bubble down a tube and (b) the motion of a single Plateau border near a wall.

of Bretherton's analysis, an expression was found which relates the thickness of the wall liquid film to the curvature of the liquid-bubble interface, the bubble slip velocity, and the ratio of surface tension and viscous stress, that is, the capillary number:

$$Ca = \frac{\mu U_{\text{slip}}}{\sigma} \quad (6)$$

When the bubble radius is large compared to the pipe diameter, the radius of curvature of the liquid-bubble interface is the pipe radius, that is $r_c = D/2$; see Figure 4. The Bretherton result is

$$\frac{1}{r_c} = \frac{3.72 Ca^{2/3}}{\delta} \quad (7)$$

and is most accurate when $Ca \rightarrow 0$. Since in our CAF system the capillary number is of order 0.05, this criterion is largely satisfied. When the single bubble

system of Bretherton is replaced by a number of contacting bubbles, Hirasaki and Lawson²⁵ argued that the appropriate radius of curvature is that of the Plateau borders formed by connecting bubbles. In 2D this radius of curvature may be derived analytically, as has been done by Princen,²³ who obtained the expression

$$r_c = 2.84a \left(\frac{\epsilon - 1}{\epsilon} \right)^{1/2} \quad (8)$$

where a is the length of thin film per bubble in contact with the pipe wall.

The stress associated with a film of thickness δ covering a fraction f of the pipe surface, sliding along on a wall with velocity u_{slip} , is

$$\tau_w = \frac{\mu U_{\text{slip}} f}{\delta} \quad (9)$$

Hence, Kraynik²² was able to obtain eq 4 by combining eqs 6–9.

When eq 4 is rearranged to give the slip coefficient for a 2D foam, the following expression is found:

$$\beta_c = \frac{218a^3 \tau_w^2 D (\epsilon - 1)^{3/2}}{\sigma^2 \mu (\epsilon^{1/2} - 3.28)^3} \quad (2D) \quad (10)$$

A treatment similar to that of Kraynik's for 3D foam may be used to obtain a 3D expression for the slip coefficient. Princen¹⁹ determined an empirical relation for f in a 3D stationary system from experiments on concentrated emulsions. The resulting empirical expression is

$$f = \frac{(\epsilon + 6.7)^{1/2} - 3.2}{(\epsilon + 6.7)^{1/2}} \quad (3D) \quad (11)$$

Following Kraynik,²² we assume that eq 11 also holds for a flowing foam.

In 3D, eq 7 remains valid for $\delta \ll D$, such that pipe curvature may be neglected. Hirasaki and Lawson²⁵ provide an expression for the Plateau border curvature in 3D, as a function of the expansion ratio, by assuming that the foam consists of pentagonal dodecahedrons. Their resulting expression is

$$\frac{r_c}{\langle R \rangle} = \frac{1.79}{\left(\epsilon^{3/2} \left(1 - \frac{1}{\epsilon} \right) \right)^{1/3}} \quad (12)$$

In combination, eqs 6, 7, 9, 11, and 12 lead to the following expression for the 3D slip coefficient:

$$\beta_c = \frac{296 \langle R \rangle^3 \tau_w^2 D (\epsilon + 6.7)^{3/2}}{\sigma^2 \mu \epsilon^{3/2} \left(1 - \frac{1}{\epsilon} \right) [(\epsilon + 6.7)^{1/2} - 3.2]^3} \quad (3D) \quad (13)$$

Equation 13 predicts that, in the limit of dry foams ($\epsilon \rightarrow \infty$), the slip coefficient is proportional to $\epsilon^{-3/2}$. It is perhaps surprising then that for our experimental conditions, that is for ϵ as low as 5.6, we observe the same dependence of the slip coefficient on ϵ .

Figure 5 shows a comparison between the slip coefficients seen experimentally by Thondavadi and Lemlich⁹ and Gardiner et al.¹⁴ and the predictions of eq 13. It seen that for the midpoint of the range of expansions used by Thondavadi and Lemlich there is a good

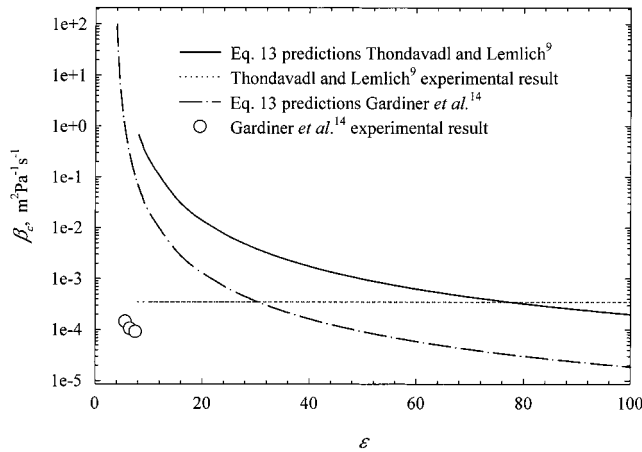


Figure 5. Comparison of slip coefficient predicted from eq 13 with the experimental results of Thondavadi and Lemlich⁹ and Gardiner et al.¹⁴ In the case of Thondavadi and Lemlich,⁹ the experimental parameters used in eq 13 were $\sigma = 0.025$ N/m, $\langle R \rangle = 500$ μm , $D = 0.044$ m, and $\tau_w = 5$ Pa, $\mu = 0.001$ Pa s, and for Gardiner et al.¹⁴ $\sigma = 0.025$ N/m, $\langle R \rangle = 80$ μm , $D = 0.01$ m, $\tau_w = 50$ Pa, and $\mu = 0.001$ Pa s.

agreement between the observed slip coefficient and the predictions of eq 13. For the results of Gardiner and co-workers a rather poor agreement is found. However these two data sets differ by the range of shear rates at which results were collected. Thondavadi and Lemlich's data were collected at low shear rates whereas those of Gardiner et al. were gathered at high shear rates.

The discrepancy seen in Figure 5 highlights a limitation of the predictive capabilities of eq 13, resulting from the assumption of an unlimited supply of liquid to form a slip layer. In reality the film thickness is limited by the ability of liquid to flow to the pipe wall to form a slip layer. When the fluid path length is greater than a single bubble layer, liquid must pass through the network of thin channels separating the bubbles. At some distance away from the wall, the resistance to flow and capillary pressures will be sufficiently high to prevent liquid from reaching the pipe wall. Let us now account for this limitation in liquid supply at high shear rates by using a simple analysis.

If we assume a uniform radial distribution of liquid within a pipe and that all the liquid available within a distance ΔR of the pipe wall ($\Delta R \ll R$) is taken to form a slip layer, the thickness of this slip layer can be expressed as

$$\delta = \frac{\Delta R}{\epsilon} \quad (14)$$

with a corresponding slip coefficient of

$$\beta_c = \frac{\Delta R D}{\epsilon \mu f} \quad (15)$$

The wall distance from which liquid is available to form a slip layer is a function of many variables including wall stress, bubble size, surface tension, and foam expansion. However, a good estimate of ΔR would be the average bubble size, as the majority of liquid is likely to come from Plateau borders in direct contact with the pipe wall. An important result from eq 15 and that presented earlier (eq 13) is that the slip layer thickness is also proportional to bubble size. Although Calvert and Nezhati's results^{17,18} did not reveal any dependence of the slip layer thickness on bubble size,

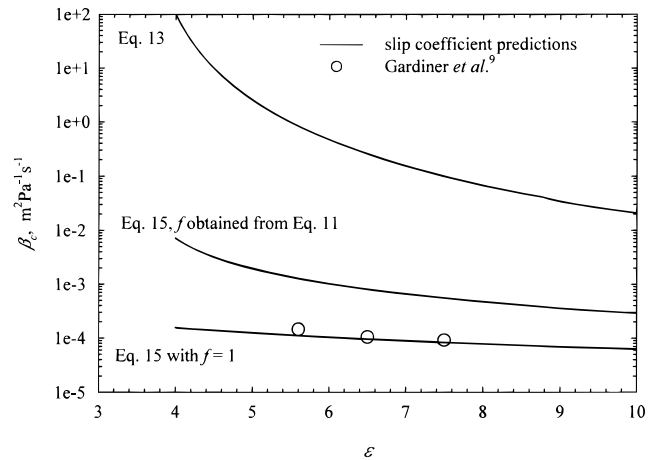


Figure 6. As the high shear rates of Gardiner et al.¹⁴ limit the rate of availability of liquid to form the slip layer, a second model, eq 15, is considered to account for restrictions on slip layer formation: $\sigma = 0.025$ N/m; $\langle R \rangle = 80$ μm ; $D = 0.01$ m; $\tau_w = 50$ Pa; $\mu = 0.001$ Pa s; $\Delta R = \langle R \rangle$.

Princen's data on concentrated emulsions showed that the fluidity indeed decreases with decreasing bubble size as expected from the above analysis. Using $\Delta R = \langle R \rangle = 80$ μm and $\epsilon = 8$, an estimate of the slip layer thickness from eq 14 is 10 μm . This estimate is typical of the slip layer thickness seen experimentally by others.^{8,9,17,18}

Figure 6 compares the prediction of eqs 13 and 15 with results found experimentally by Gardiner et al.¹⁴ The values of parameters used are typical of experimental conditions. It is clearly seen in Figure 6 that excellent agreement for the slip coefficient is obtained when the slip layer thickness is limited according to eq 14 and the Plateau borders near the surface are assumed to be entirely depleted of liquid ($f = 1$). Thus it can be concluded that eqs 13 and 15 apply at low and high shear rates, respectively, reflecting the different formation mechanisms of the slip layer.

Equations To Predict Pressure Losses in Pipes

The results of the previous two sections have placed us in a position to predict pressure losses of foam flowing through pipes. The first step in the procedure is to derive the general pipe flow equations using a volume-equalized power-law viscosity model. In treating the flow of foam through pipes, we consider the gas phase to be compressible and the liquid phase to be incompressible. We also assume no relative motion of phases within the bulk foam, allowing the foam to be treated as a single phase fluid. The assumption of no relative motion between phases is less likely to hold when the liquid fraction approaches unity. There is no mass transfer between phases, and the gas-phase obeys the ideal gas law. It is also assumed that the gas within the foam undergoes isothermal expansion.

Equation 16 represents the volume equalized power-law model of foam viscosity, where the shear stress is

$$\frac{\tau}{\epsilon} = - \frac{k}{\epsilon} \left| \frac{dv}{dr} \right|^{n-1} \frac{dv}{dr} = k \left(- \frac{dv}{\epsilon dr} \right)^n \quad (16)$$

given by eq 17 if small inertial effects are neglected.²⁶

$$\tau = - \frac{r(dP)}{2(dx)} \quad (17)$$

Combining eqs 16 and 17 and then integrating with the wall slip boundary condition $r = R$, $v = u_{\text{slip}}$, we obtain

$$v = u_{\text{slip}}(\epsilon) + \frac{nR^{(1+n)/n}}{1+n} \left(-\frac{1}{2k} \left(\frac{dP}{dx} \right) \epsilon^{n-1} \right)^{1/n} \left[1 - \left(\frac{r}{R} \right)^{(1+n)/n} \right] \quad (18)$$

Equation 18 gives the velocity profile of the foam pipe flow. The volumetric flow rate is equal to the average velocity multiplied by the cross sectional area. The mass flow rate is constant and equivalent to the product of the volumetric flow rate and foam density; that is,

$$Q = \pi R^2 \left\{ u_{\text{slip}}(\epsilon) + \left[-\left(\frac{n}{3n+1} \right)^n \left(\frac{\epsilon^{n-1}}{2k} \right) R^{1+n} \left(\frac{dP}{dx} \right)^{1/n} \right] \right\} \quad (19)$$

Rearranging eq 19 we obtain

$$\int_{P_0}^P -\frac{R^{n+1}}{2k\epsilon^{1-n}} \left[\frac{3n+1}{n} \left(\frac{Q}{\pi R^2} - u_{\text{slip}}(\epsilon) \right) \right]^{-n} dP = \int_0^L dx \quad (20)$$

It can be shown²⁷ that

$$\left(\frac{dP}{dx} \right) = \frac{NP\epsilon^2}{\rho_L(\epsilon-1)} \quad (21)$$

where the polytropic expansion exponent N is unity for isothermal expansion and 1.4 for adiabatic expansion of diatomic gases.

In eq 21, it is assumed that $m_L \gg m_G$. Note that

$$\frac{d\epsilon}{dP} = -\frac{\rho_L}{\rho^2} \frac{d\rho}{dP} = -\frac{\epsilon-1}{NP} \quad (22)$$

Integrating eq 22, with the condition of $P = P_0$ at $\epsilon = \epsilon_0$ and the approximation of isothermal expansion, results in the following expression:

$$\frac{P}{P_0} = \frac{\epsilon_0 - 1}{\epsilon - 1} \quad (23)$$

By solution of eq 20 with the help of eq 23, a pressure drop for a given length of pipe may be found for various foam expansions. Note that eq 20 can only be solved for pipes for which there is a known relationship between u_{slip} and ϵ . For our system, the dependence of ϵ on the slip velocity is given in Figure 2.

As eq 20 has no obvious analytical solution, it was solved numerically using the bisection method. In particular a numerical solution was found to

$$F(\Delta P_i) = \frac{-R^{n+1}}{2k\epsilon_{i-1}^{1-n}} \left[\frac{3n+1}{n} \left(\frac{Q}{\pi R^2} - u_{\text{slip}}(\epsilon_{i-1}) \right) \right]^{-n} \Delta P_i - \Delta x_i \quad (24)$$

for a given Δx_i , such that $F(\Delta P_i) = 0$, where the subscript i denotes parameters relating to the i th equation and the i th solution. The pressure and specific expansion are then updated according to eqs 25 and 26, and the

$$P_i = P_{i-1} + \Delta P_i \quad (25)$$

$$\epsilon_i = \frac{P_{i-1}(\epsilon_{i-1} - 1)}{P_i} + 1 \quad (26)$$

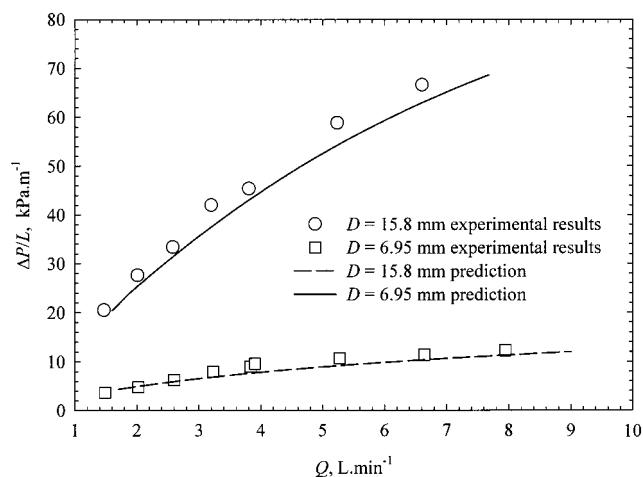


Figure 7. Comparison of the pressure loss predictions of eq 20 with Gardiner et al.'s¹⁴ $\epsilon_{\text{mid}} = 6.5$ flow data for two pipe diameters and gauge pressure of 340 kPa. The slip velocity was determined from the ϵ -dependent scaling curve found in Figure 3.

process is repeated for the new variables, where $u_{\text{slip}}(\epsilon_i)$ is determined from either experimental data or the slip models presented in the previous section. The final pressure drop along the pipe length is found by the ratio of eqs 27a and 27b, that is $\Delta P/L$.

$$L = \sum_i \Delta x_i \quad \Delta P = \sum_i \Delta P_i \quad (27a,b)$$

Prediction Results and Discussion

To test the predictive capability of eq 20, the experimental conditions of Gardiner et al.¹⁴ are incorporated into eq 20. In particular the ambient pipe pressure, specific expansion ratio, pipe diameter, and volume equalized power-law indices are used for each set of predictions. As the specific expansion ratio and pressure were only determined by Gardiner et al.¹⁴ at a single point along the pipe length ($x = L/2$), the specific expansion at the entrance of the pipe ϵ_0 is not known. Therefore when pressure losses are predicted for ϵ_{mid} , an initial guess was made for P_0 and ϵ_0 . The estimates of P_0 and ϵ_0 are then adjusted until eq 20 produces $P = P_0$ and $\epsilon = \epsilon_0$ at $x = L/2$. This iterative procedure is only necessary so that model predictions can be compared directly with available experimental data for this paper. In practice P_0 and ϵ_0 are starting conditions for eq 20, chosen for the foam application of interest.

Figures 7 and 8 present the experimental results of Gardiner et al.¹⁴ compared with the predictions of eq 20, for $\epsilon_{\text{mid}} = 6.5$ and 7.5 and pipe diameters of 6.95 and 15.8 mm at gauge pressures of 340 kPa. The slip velocity used in eq 20 was obtained using the line of best fit featured in Figure 3, which incorporates the dependence of the slip velocity on ϵ . It is seen that for all cases the predictions agree with experimental points to within 15%, and in some instances it is less than 5%. The largest error occurs when there is the greatest pressure drop, that is for the smallest pipe diameter $D = 6.95$ mm. The pressure loss prediction is sensitive to the slip velocity determination, which in turn is sensitive to pressure changes. If the foam is pumped at very high pressures and the pressure drop along the pipe is relatively small, then the dependence on ϵ on the integration of the left-hand side of eq 20 can be neglected.

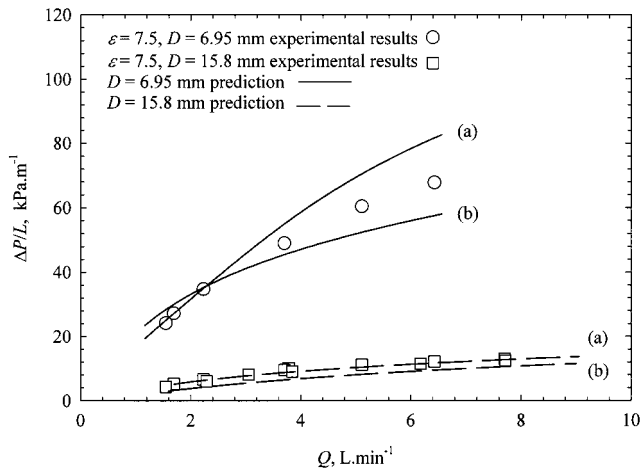


Figure 8. Comparison of the pressure loss predictions of eq 20 with Gardiner et al.'s¹⁴ $\epsilon_{\text{mid}} = 7.5$ flow data for two pipe diameters and gauge pressure of 340 kPa. The slip velocity was determined by (a) the ϵ -dependent scaling curve found in Figure 3, and (b) the predictions of eq 15 with $f = 1$.

As seen earlier, eq 15 may be used to calculate a slip coefficient, from which one can obtain a slip velocity using eq 1. Figure 8 includes pressure loss predictions obtained using a slip velocity determined from eqs 15 ($f = 1$) and 1. Pressure loss predictions, obtained using this alternate method, agree with experiments to a similar accuracy as the ϵ -dependent evaluation, that is $\sim 15\%$. Figure 8 also highlights the sensitivity of predictions to the accuracy of the slip model.

The application of the above theory of foam flow is restricted to conditions over which there is no significant change in either the rheology of the foam and, possibly of greater importance, no change in the form of the slip layer. These restrictions would be favored by short pipe lengths, high pressures, and where the stable lifetime of the foam is much longer than the characteristic time scale of the foam pipe transit time. If the foam drains considerably within the pipe, it could be expected that the slip layer may vary in thickness around the circumference of the pipe and two phase flow will develop. An asymmetry in the slip layer due to drainage could not be observed in the systems of Enzendorfer et al.¹² or Gardiner et al.¹⁴ due to the use of stainless steel pipes because of elevated pressures in the experiments. For Gardiner et al.'s¹⁴ system the foam drainage time is much longer than the foam-pipe transit time, and so no significant drainage should occur within the pipe rheometer.

Finally from a practical perspective, the results of this paper form the basis for the development of standard calculations for designing pipe networks for the transport of foams (e.g. developing foam-sprinkler fire suppression systems). The calculations presented in this paper apply only to straight pipe sections and require foam viscosity and slip models which presently need to be determined empirically. The flow behavior in bends and T-sections is complex and has not yet been simulated, but it is known from practice that foam may undergo dramatic changes in its structure, including the complete breakdown of the foam matrix and separation.² Thus further research on foam flows through bends and T-sections is required for the development of complete algorithms for pressure drops in pipe networks.

Conclusions

With the recent widespread use of aqueous foams, there is a need for predicting the pressure losses associated with the flow of foam through pipes at elevated pressures. The method of volume equalization allows a foam to be characterized by a single viscosity model over a range of pipe pressures and expansions once the properties of the foam have been established at a single expansion and pressure. It has been found that the following equation, based on the method of volume equalization, allows the prediction of pressure losses in flowing foam in pipes:

$$\int_{P_0}^P \frac{R^{n+1}}{2k\epsilon^{1-n}} \left[\frac{3n+1}{n} \left(\frac{Q}{\pi R^2} - u_{\text{slip}}(\epsilon) \right) \right]^{-n} dP = \int_0^L dx$$

This equation requires a knowledge of the functional dependence of the slip velocity on the specific expansion ratio, since the bulk flow of foam and the foam slip at the pipe wall are coupled. Wall slip plays a significant role in the flow behavior of foams. Two models are presented to predict slip velocities. The first of these is suitable for low flow rates, where the rate of liquid transport through Plateau borders to the pipe wall is sufficient to allow complete formation of the slip layer. The low-shear slip coefficient may be expressed as

$$\beta_c = \frac{296 \langle R \rangle^3 \tau_w^2 D (\epsilon + 6.7)^{3/2}}{\sigma^2 \mu \epsilon^{3/2} \left(1 - \frac{1}{\epsilon} \right) [(\epsilon + 6.7)^{1/2} - 3.2]^3}$$

The second model of wall slip applies when the foam flow rate is high and the formation of the slip layer is restricted by the availability of liquid close to the pipe wall. In this case, the slip coefficient is described by the following equation:

$$\beta_c = \frac{\Delta R D}{\epsilon \mu f}$$

Using these expressions, good agreement is found between the calculated and experimental results from data sets available for comparison in the literature.

Acknowledgment

Discussions with Dr. Andrew Kraynik of Sandia National Laboratories are acknowledged with gratitude.

Nomenclature

- a = length of thin film in contact with pipe wall in 2D (m)
- c = velocity of sound (m s^{-1})
- D = pipe diameter (m)
- E = expansion ratio, volume of foam/volume foam solution at atmospheric conditions
- f = fraction of pipe surface covered by thin films
- k = power law constant (Pa s^n)
- L = pipe length (m)
- m_L, m_G = liquid and gas mass flow rates respectively (kg s^{-1})
- N = polytropic expansion exponent
- n = power law index
- P = pressure in the pipe (Pa)
- Q = volumetric flow rate ($\text{m}^3 \text{s}^{-1}$)
- R = pipe radius (m)
- r = denotes pipe radial coordinate (m)
- $\langle R \rangle$ = average bubble radius (m)

r_c = radius of curvature of a Plateau border (m)
 u_{slip} = slip velocity (m s⁻¹)
 V_G, V_L = volume of gas- and liquid-phases, respectively (m³)
 v = foam velocity (m s⁻¹)
 x = denotes pipe axial coordinate (m)
 β_c = corrected slip coefficient (fluidity) (m² Pa⁻¹ s⁻¹)
 β_{ce} = corrected slip coefficient independent of specific expansion ratio (m² Pa⁻¹ s⁻¹)
 δ = thickness of liquid slip layer (m)
 ϵ = specific expansion ratio at in situ conditions, ρ_L/ρ
 ϵ_{mid} = specific expansion ratio at midpoint of pipe, $\epsilon_{\text{mid}} \approx \epsilon$
 $(\dot{\gamma}_{\text{aw}})_{\text{True}}$ = apparent/Newtonian shear rate with the effects of wall slip removed (s⁻¹)
 μ = viscosity of foam solution (Pa s)
 ρ_L, ρ = density of foam solution and density of foam at in situ conditions (kg m⁻³)
 σ = gas-liquid surface tension (N m⁻¹)
 τ = shear stress (Pa)
 τ_y = yield stress (Pa)

Literature Cited

- (1) Liebson, J. *Introduction to Class A Foams and Compressed-Air Systems for the Structural Fire Service*, ISFSI: Ashland, MA, 1991.
- (2) Kim, A. K.; Dlugogorski, B. Z. Multipurpose Overhead Compressed-Air Foam System and Its Fire Suppression Performance. *J. Fire Prot. Engr.* **1997**, *8*, 133.
- (3) Aubert, J. H.; Kraynik, A. M.; Rand, P. B. Aqueous Foams. *Sci. Am.* **1986**, *254*, 58.
- (4) Oldroyd, J. G. The Interpretation of Observed Pressure Gradients in Laminar Flow of Non-Newtonian Liquids Through Tubes. *Colloid Sci.* **1949**, *4*, 333.
- (5) Jastrzebski, Z. Entrance Effect and Wall Effects in an Extrusion Rheometer during the Flow of Concentrated Suspensions. *Ind. Eng. Chem. Res.* **1967**, *6*, 445.
- (6) Valkó P.; Economides, M. Volume Equalized Constitutive Equations for Foamed Polymer Solutions. *J. Rheol.* **1992**, *36*, 1033.
- (7) Heller, J.; Kuntamukkula, M. Critical Review of Foam Rheology Literature. *Ind. Eng. Chem. Res.* **1987**, *26*, 318.
- (8) Wenzel, H. G.; Brungraber, R. J.; Stelson, T. E. The Viscosity of High Expansion Foam. *J. Mater. JMLSA* **1970**, *5*, 396.
- (9) Thondavadi, N. N.; Lemlich, R. Flow Properties of Foam With and Without Solid Particles. *Ind. Eng. Chem. Process Des. Dev.* **1985**, *24*, 748.
- (10) de Krasinski, J.; Fan, Y. Some Viscoelastic Aspects of Liquid Foams of High Void Fraction and Possibilities of their Applications. *XVIIth Int. Congr. Theor. Appl. Mech. (ICTAM)* **1984**, 463.
- (11) Khan, S. A.; Schnepfer, C. A.; Armstrong, R. C. Foam Rheology: III. Measurement of Shear Flow Properties. *J. Rheol.* **1988**, *32*, 69.
- (12) Enzendorfer, C.; Harris, R. A.; Valkó, P.; Economides, M. J.; Fokker, P. A.; Davies, D. D. Pipe Viscometry of Foams. *J. Rheol.* **1995**, *39*, 345.
- (13) Boissonnet, G.; Faury, M.; Fournel, B. Decontamination of Nuclear Components through the Use of Foams. Presented at NATO School on Foams, Emulsions and Cellular Structures, Cargèse, May 1997.
- (14) Gardiner, B. S.; Dlugogorski, B. Z.; Jameson, G. J. Rheology of Fire-Fighting Foams. *Fire Safety J.* **1998**, *31*, 61.
- (15) Gardiner, B. S.; Dlugogorski, B. Z.; Jameson, G. J., Chhabra, R. P. Yield Stress Measurements of Aqueous Foams in the Dry Foam Limit. *J. Rheol.* **1998**, *42*, 1437.
- (16) Yoshimura, A. S.; Prud'homme, R. K.; Princen, H. M., Kiss, A. D. A Comparison of Techniques for Measuring Yield Stresses. *J. Rheol.* **1987**, *31*, 699.
- (17) Calvert, J. R.; Nezhati, K. A Rheological Model for a Liquid-Gas Foam. *Int. J. Heat Fluid Flow* **1986**, *7*, 164.
- (18) Calvert, J. R.; Nezhati, K. Bubble Size Effects in Foams. *Int. J. Heat Fluid Flow* **1987**, *8*, 102.
- (19) Princen, H. M. Rheology of Foams and Highly Concentrated Emulsions II. Experimental Study of the Yield Stress and Wall Effects for Concentrated Oil-in-Water Emulsions. *J. Colloid Interface Sci.* **1985**, *105*, 150.
- (20) Mooney, M. Explicit Formulas for Slip and Fluidity. *J. Rheol.* **1931**, *2*, 210.
- (21) Gardiner, B. S.; Dlugogorski, B. Z.; Jameson, G. J. Behaviour of foams in tubular flow. *Proceedings of the 2nd Pacific Rim Conference on Rheology (PRCR2)*; Monash University Printing Services: Melbourne, July 1997; p 75.
- (22) Kraynik, A. M. Foam Flows. *Annu. Rev. Fluid Mech.* **1988**, *20*, 325.
- (23) Princen, H. M. Highly concentrated emulsions I. Cylindrical systems. *J. Colloid Interface Sci.* **1979**, *71*, 55.
- (24) Bretherton, F. P. The Motion of Long Bubbles in Tubes. *J. Fluid Mech.* **1961**, *10*, 166.
- (25) Hirasaki, G. J.; Lawson, J. B. Mechanisms of Foam Flow in Porous Media: Apparent Viscosity in Smooth Capillaries. *Soc. Pet. Eng. J.* **1985**, *25*, 176.
- (26) Wenzel, H. G., Stelson, Brungraber, R. J. Flow of High Expansion Foam in Pipes. *Proc. Am. Soc. Civ. Eng.* **1967**, *EM6*, 153.
- (27) Wood, A. B. *A Textbook of Sound*; Bell: London, 1941.

Received for review June 16, 1998

Revised manuscript received November 19, 1998

Accepted November 30, 1998

IE980385I